# DEVELOPMENT OF NIOBIUM SPUTTERING APPARATUS AT KEK

R. Katayama*, T. Saeki, T. Kubo, H. Hayano, H. Ito,
High Energy Accelerator Research Organization, Tsukuba, Japan
Y.Iwashita, Kyoto University, Osaka, Japan,
R.Ito, T. Nagata, ULVAC inc., Chiba, Japan

*Abstract*

We developed a novel Nb sputtering apparatus to coat the interior of a 3-GHz elliptical cavity and study the S′IS structure. This DC magnetron sputtering apparatus allowed the synthesis of Nb and NbN thin films on the inner surfaces of the 3-GHz SRF cavity. The theory predicts that a bi-layer structure comprising dirty Nb or NbN on pure bulk Nb as an S′S structure, i.e., the special case of the thickness of the I layer 0, can also enhance the maximum acceleration gradient better than the ordinal Nb SRF cavity. Accordingly, we report the characteristics of this apparatus and details of its development.

## INTRODUCTION

The maximum acceleration gradient of a superconducting radiofrequency cavity is limited by the surface magnetic field at which a vortex avalanche occurs (effective Hc1). This theory predicts that the effective Hc1 can be pushed up by the superconductor–insulator–superconductor structure(S′-I-S structure) [1–4]. Experimental results demonstrate that an S′IS structure comprising NbN, $SiO_2$, and pure bulk Nb significantly enhances the effective Hc1 [5–7]. The film formation technique is the key to realizing a next-generation SRF cavity coated with an S′IS structure. Hence, the KEK-ULVAC collaboration developed a film formation technique for S′IS structures [8–10]. In addition, we developed a novel Nb-sputtering apparatus to coat the interior of an elliptical cavity. This DC magnetron sputtering apparatus enabled the synthesis of Nb and NbN thin films on the inner surfaces of the SRF cavity. The theory predicts that even if such bi-layer structure comprises dirty Nb or NbN on pure bulk Nb as an S′S structure, i.e., the special case of the thickness of I layer 0, the maximum acceleration gradient is enhanced better than the ordinal Nb SRF cavity [3]. We report the characteristics of this apparatus, the details of the system's development, and the obtained results.

## APPARATUS

DC magnetron sputtering was employed as the film formation technique. The schematic of the apparatus is presented in Fig. 1. This apparatus comprises a vacuum chamber, a niobium cathode with a permanent magnet, and an inlet for argon and nitrogen gas flow. The cathode rod was mounted at the center of the vacuum chamber. Plasma was induced around the rod by supplying argon gas and applying a DC voltage to the rod. The ions attracted by the negative DC voltage kick out Nb particles from the cathode into the interior of the SRF cavity surface. We can also supply a gas mixture of argon and nitrogen instead of argon. Here, NbN thin films can be synthesized on cavity surfaces. In general, DC magnetron sputtering depends on several film-formation parameters, such as the incident angle of the niobium particles scattered onto the cavity surface, gas flow rate, gas pressure, electric and magnetic fields, and temperature of the substrate. However, the film formation parameters inside the cavity continuously change depending on their position. Hence, the optimization of the DC magnetron sputtering process inside the cavity should be considered more difficult than that of the ordinal-plane-shaped substrate. Hence, we prepared a 3-GHz coupon cavity to investigate the dependence of the film thickness and film quality on various positions inside the cavity (see Fig. 2) [11, 12]. We adopted two models, Nb and Cu, for the coupon cavities. In addition, we prepared coin samples made of Nb and Cu ($\phi$-20 mm), which could be attached to holes on the surface of the coupon cavity [11, 12]. Using a coupon cavity with coin samples, we can evaluate the position dependence of the quality of the synthesized film via several surface analyses. For example, we can evaluate the effective Hc1 using the third harmonic voltage method for a sample taken from a coupon cavity after synthesizing the films [7].

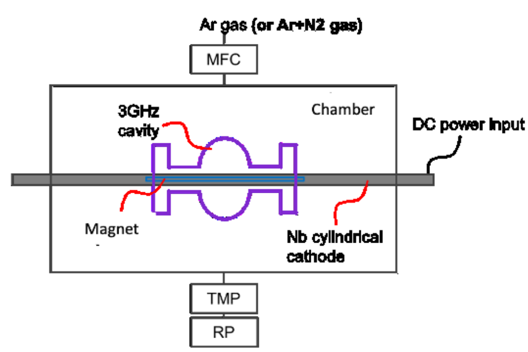


Figure 1: Schematic diagram of the niobium sputtering apparatus.

## EXPERIMENTAL RESULT

We conducted tests on DC magnetron sputtering against coupon cavities and coin samples in 2020 and 2023.5.17 to 5.19. Glass plate samples were employed to evaluate the thicknesses of the Nb-sputtered films. The obtained results are described in the following section.

* ryo.katayama@kek.jp

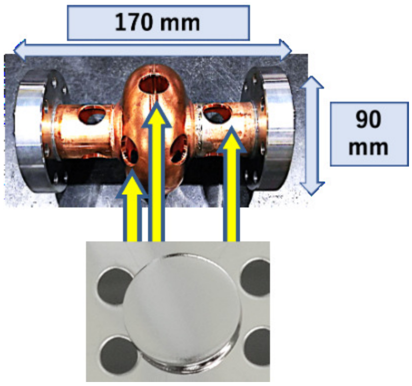


Figure 2: Photograph of 3-GHz coupon cavity made of Cu and Nb coin sample.

### *Experiment (2020)*

In 2020, we conducted DC magnetron sputtering tests at Tigold Inc. against the Cu coupon cavity to which Cu coin samples were attached. The apparatus described in the previous section was mounted in the vacuum chamber of a Tigold Inc. production machine. After vacuum pumping, argon gas (0.65 Pa) was supplied to the Nb cathode while a 0.5-kW DC power was applied to the Nb cathode. We verified that DC magnetron sputtering occurred in the chamber, resulting in a Nb thin-film deposition on the cavity surface. Images of the interior of the Cu coupon cavity and Cu coin sample after the film formation are presented in Fig. 3. A Nb thin film was deposited on the entire surface of the Cu coupon cavity without peeling. In addition, no peeling of the synthesized films from the Cu coin samples was observed. In contrast, peeling was observed near the part between the beam pipe and NbTi flange weld. Subsequently, we roughed the surface using sandpaper because there was a possibility that these peelings could have been caused by contamina-tion and the effect of surface roughness. Accordingly, the adhesion was significantly improved, and no peeling was observed. Images of the interior of the Cu coupon cavity after the sputtering process before and after roughing with sandpaper are presented in Fig. 4.

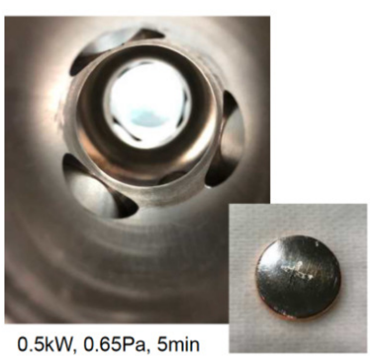


Figure 3: Photograph of the interiors of the Cu coupon cavity and Cu coin sample after DC magnetron sputtering.

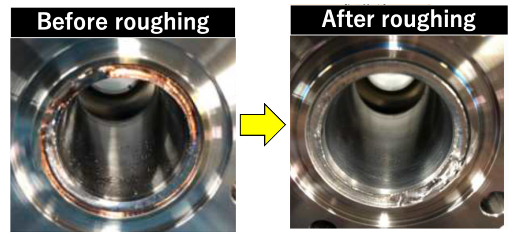


Figure 4: Comparison of the NbTi flange after DC magnetron sputtering before and after roughening the surface with the sand paper.

### *Experiment (2023.5.17-5.19*

DC magnetron sputtering tests with Cu and Nb coupon cavities were conducted again at the Tigold facility from 17-05-2023 to 19-05-2023. 0.5-kW DC power and 0.67-Pa argon gas pressure were employed, same as the previous test conducted in 2020. The Nb coin samples adopted in this test were as follows: (1) Nb coin samples as received and (2) Nb coin samples to which mechanical polishing, 800 °C for 3-h anneal, and EP were applied. On 05-17-2023, Nb sputtering test was conducted. It was verified that this test reproduced previous results. Moreover, the uniformity of the film thickness distribution improved (as discussed later). On May 18, 2023, the plasma could not be suddenly induced in the vacuum chamber. After inspecting the interior of the Nb cathode, we inferred that the magnetism of the neodymium magnet was lost. Hence, we replaced the neodymium magnets with new magnets. Subsequently, we could induce plasma sputtering again in the chamber using a cathode with replaced magnets. On May 19, 2023, we first performed DC magnetron sputtering of a Cu coupon cavity using as-received Nb coin samples and two polished Nb coin samples. Subsequently, we sputtered the Nb coupon cavity with three glass plates and 12 as-received Nb coin samples. No peeling was observed during the sputtering test of the Cu coupon cavity. In contrast, in the Nb coupon cavity, peeling was observed near the edge of the beam-pipe tube (Fig. 5). In addition, pits were observed on the surfaces of the two polished niobium coin samples attached to the Cu coupon cavity (Fig. 6 and Fig. 7), whereas there was no pit on the surfaces of the as-received Nb coin samples. We finally performed DC magnetron sputtering of a Cu coupon cavity using 12 as-received Nb coin samples and three glass plates under 0.3 kW DC power and 0.67-Pa argon gas pressure for 10 min.

### *Comparison of Film Thickness Distribution*

A comparison of the Nb film thickness distribution at several points on the 3-GHz coupon cavity is summarized in Fig. 8. The uniformity obtained on May 17, 2023 is improved compared to that obtained in 2020. The thickness of the synthesized films increased as the position changed from the equator to the iris. The grown rate of Nb film thickness increased as DC power becomes higher.


Figure 5: Photograph of the position near the beam pipe tube of the Nb coupon cavity after DC magnetron sputtering.

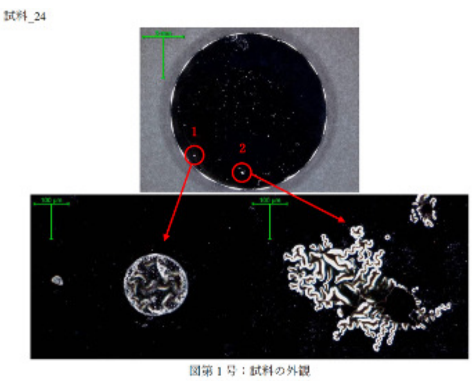


Figure 6: (TOP) Photograph of Nb coin Sample 1 after DC magnetron sputtering. (Bottom) Enlarged image near the pits on the Nb coin surface.

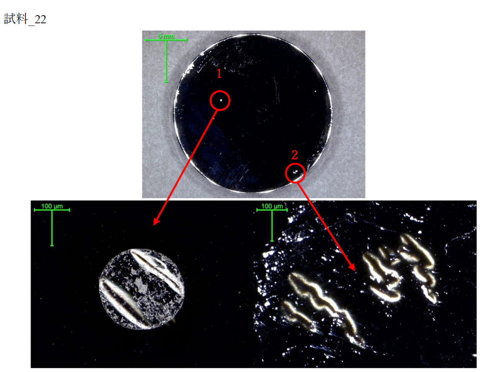


Figure 7: (TOP) Photograph of Nb coin Sample 2 after DC magnetron sputtering. (Bottom) Enlarged image near the pits on the Nb coin surface.

*Analyses Result of SEM-EDS*

We performed SEM-EDS measurements on samples of the peeled films collected from the Nb coupon cavity. The obtained results are presented in Fig. 9. In the SEM-EDS spectrum, the horizontal and vertical axes represent the X-ray energy and number of photons, respectively. Almost all Nb signals were observed; however, small carbon and oxygen peaks were also emerged. In addition, we performed SEM-EDS measurements on two polished Nb coin samples. The obtained results are presented in Fig. 10, Fig. 11, Fig. 12, and Fig. 13. Almost all the Nb signals were observed; however, a small oxygen peak appeared.

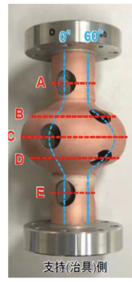


Unit: nm

| | 2020 (500 W, 5 min) | 2023.5.17 (500 W, 5 min) | 2023.5.19 (500 W, 5 min) | 2023.5.19 (300 W, 10 min) |
|---|---|---|---|---|
| A | 818.0 | 655.7 | 684.6 | 927.9 |
| C | 234.9 | 228.5 | 210.7 | 298.4 |
| E | 679.0 | 665.7 | 568.5 | 823.2 |

Figure 8: Comparison of film-thickness distribution on various positions of Cu coupon cavity between the experiments in 2020 and 2023. A and E correspond to the iris position, whereas C corresponds to the equator.

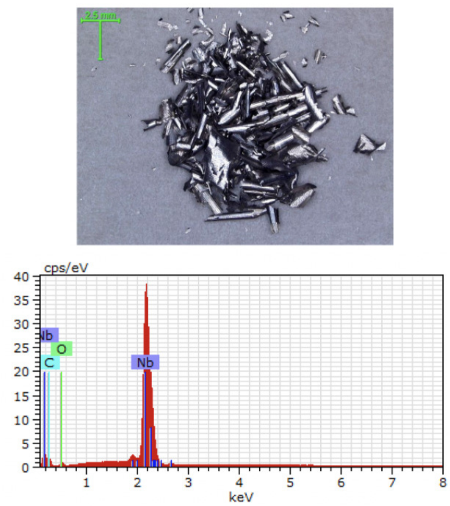


Figure 9: SEM-EDS spectrum of the sample collected from peeled films of Nb coupon cavity in Fig. 5.

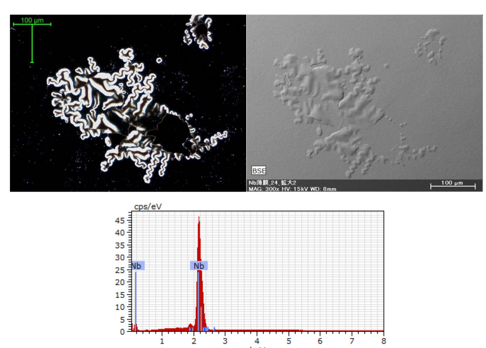


Figure 10: SEM-EDS spectrum on the pit of the Nb coin sample in Fig. 6.

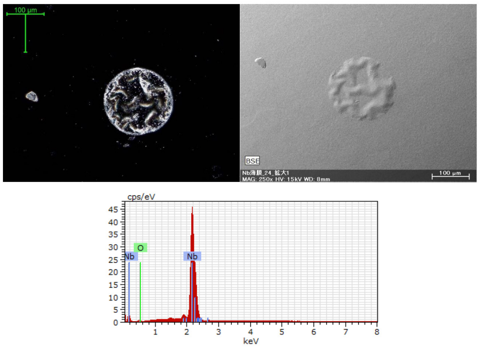


Figure 11: SEM-EDS spectrum on the pit of the Nb coin sample in Fig. 6.

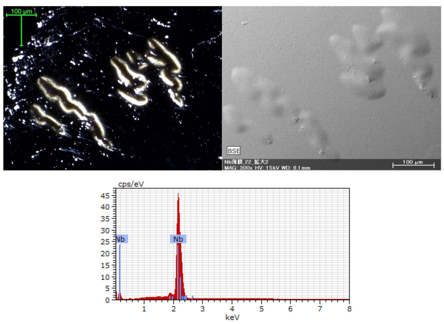


Figure 12: SEM-EDS spectrum on the pit of the Nb coin sample in Fig. 7.

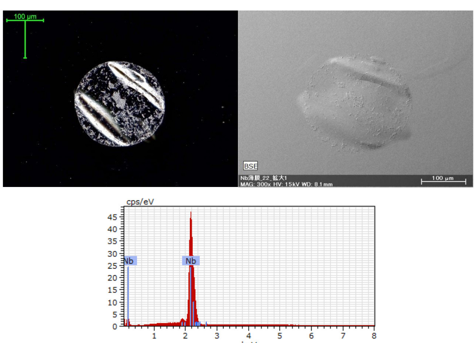


Figure 13: SEM-EDS spectrum on the pit of the Nb coin sample in Fig. 7.

## DISCUSSION

No surface or heat treatment was applied to the Nb coupon cavity. In general, surface contamination causes film peeling problems. Hence, in the future, chemical- or electropolishing should be applied to the Nb coupon cavity prior to DC magnetron sputtering. In addition, gas emissions, scratches, and/or dust triggered pits on the surfaces of the Nb coin samples after film coating. However, dust was most likely eliminated from the candidates because there were no strong peaks other than those of the Nb in SEM-EDS. The lack of a baking process may trigger gas emission during DC magnetron sputtering, and mechanical polishing may cause scratches on the surfaces. Therefore, it is desirable to prepare Nb coin samples without mechanical polishing and by baking process at 100-200 °C for several hours, to suppress scratching and gas emissions during DC magnetron sputtering.

## SUMMARY

We developed a DC magnetron sputtering apparatus to coat a 3-GHz SRF cavity for a film formation study of the S′IS structure. A niobium thin film can be formed inside the 3-GHz coupon cavity. Using this apparatus, we can synthesize a bilayer structure inside a pure bulk Nb cavity.

## ACKNOWLEDGMENTS

This work was performed by ULVAC-KEK Collaboration Project Number 2018-C315 and 2019-C315. This work was supported by Toray Science Foundation Grant No.19-6004 and Japan Society for the Promotion of Science (JSPS) KAKENHI Grant Numbers JP17H04839, JP19H04395, and JP23H00125. I am grateful to Masaki Ishida of Applied Research Laboratory Radiation Science Center at KEK for chemical analysis with measuring SEM-EDS.

## REFERENCES

[1] A. Gurevich, "Enhancement of rf breakdown field of superconductors by multilayer coating", Appl. Phys. Lett. 88, 012511 (2006).

[2] T. Kubo *et al.*, "Radio-frequency electromagnetic field and vortex penetration in multilayered superconductors", Appl. Phys. Lett. 104, 032603 (2014).

[3] T. Kubo, "Multilayer coating for higher acceleration fields in superconducting radio-frequency cavities: a review of theoretical aspects", Supercond. Sci. Tech-nol. 30, 023001 (2017).

[4] T. Kubo, "Superheating fields of semi-infinite superconductors and layered superconductors in the diffusive limit: structural optimization based on the microscopic theory", Supercond. Sci. Technol. 34 045006 (2021).

[5] R. Katayama *et al.*, "Evaluation of superconducting characteristics on the thin-film structure by NbN and Insulator coatings on pure Nb substrate", IPAC2018 Proceedings, Vancouver, Canada, pp.3653–3655.

[6] R. Katayama *et al.*, "Precise Evaluation of Characteristic of the Multi-layer Thin-film Superconductor Consisting of NbN and Insulator on Pure Nb Substrate", LINAC2018 Proceedings, Beijing, China, pp.391–394.

[7] R. Katayama *et al.*, "Evaluation of the superconducting characteristics of multi-layer thin-film structures of NbN and SiO2 on pure Nb substrate", SRF2019 Proceedings, Dresden, Germany, pp.807–809.

[8] R. Ito, T. Nagata *et al.*, "Development of Coating Technique for Superconducting Multilayered Structure", IPAC2018 Proceedings, Vancouver, Canada, pp.4954–4956.

[9] R. Ito, T. Nagata *et al.*, "Construction of Thin-film Coating System Toward the Realization of Superconducting Multilayered Structure", LINAC18 Proceedings, Beijing, China, TUPO050, pp.445–447.

[10] R. Ito, T. Nagata, H.Hayano, R.Katayama, T.Kubo, S.Takayuki *et al.*, "$Nb_3Sn$ Thin Film Coating Method for Superconducting Multilayered Structure", SRF2019 Proceedings, Dresden, Germany (2019), pp.628–631.

[11] T. Saeki, H. Hayano, T. Kubo, H. Inoue, R. Katayama, F. E. Hannon, R. Rimmer, Y. Iwashita, H. Tongu, H. Ito, "Fabrication of 3.0-GHz Single-cell Cavities for Thin-film Study", SRF2019, MOP054, pp.177–181.

[12] Y. Iwashita, Y. Kuriyama, H. Tongu, Y. Fuwa, H. Hayano, H. Ito, R. Katayama, T. Kubo, T. Saeki, "Instrumentation R&D at KEK and Kyoto University", SRF2021, TUPFDV008, pp.421–425.